GaAs HEMT Monolithic Voltage-Controlled Oscillators at 20 and 30 GHz Incorporating Schottky-Varactor Frequency Tuning

Oya Sevimli, *Member, IEEE,* John W. Archer, *Fellow, IEEE,* and Grant J. Griffiths, *Member, IEEE*

***Abstract*— This paper describes the design and fabrication of fully monolithic voltage-controlled oscillator (VCO) circuits using a combined GaAs high electron-mobility transistor (HEMT) and Schottky-varactor diode process. To the authors' knowledge, this is the first time a process of this type has been used for VCO fabrication. Three VCO designs with similar circuit topology, but two different operating frequencies and resonator types, were investigated to compare their relative performance. Two approaches to the integrated resonator were tried: coupled and single microstrip lines. The single resonator approach resulted in better power efficiency, while the coupled resonator was found to provide a wider frequency tuning range and lower phase noise.**

***Index Terms*— High electron-mobility transistor, monolithic-microwave integrated circuit, Schottky-varactor diode, voltage-controlled oscillator.**

I. Introduction

THERE have been many monolithic or quasi-monolithic oscillators reported in the technical literature [1]. Most of these use MESFET or heterojunction bipolar transistor (HBT) devices because oscillators using such devices have been shown to produce lower phase noise than high electron-mobility transistor (HEMT)-based oscillators. However, high-performance HEMT oscillators are essential if they are to be integrated with HEMT amplifiers and mixers for single-chip receivers or transmitters. Recently, with this goal in mind, successful HEMT oscillators operating at higher microwave and millimeter-wave frequencies have been reported [2], [3].

In the voltage-controlled oscillator (VCO) circuits described in this paper, an HEMT device is used to provide negative resistance to start and maintain oscillation, and a variable capacitance provides frequency tuning. The wide range of capacitance versus dc-bias voltage available from a Schottky-varactor diode increases the frequency coverage of the VCO and provides more linear frequency tuning than would be available if a diode based on an HEMT epitaxial structure was used in place of the varactor. Combining HEMT and Schottky-varactor diode technologies on a single wafer enables the development of fully monolithic VCO's with a wide-frequency coverage at microwave and millimeter-wave frequencies.

Manuscript received October 25, 1997; revised May 15, 1998.

The authors are with the Commonwealth Scientific and Industrial Research Organization, Telecommunications and Industrial Physics, Marsfield, N.S.W. 2122, Australia.

Publisher Item Identifier S 0018-9480(98)06730-1.

A fully monolithic VCO requires an integrated resonator. Many different resonator types are realizable in microstrip form: e.g., ring [4], coupled, or single resonators [5]. These resonators are easily integrated with the VCO circuit at higher microwave or millimeter-wave frequencies. In choosing the resonator type, consideration must be given to the quality (Q) factor and its influence on two important performance characteristics: higher Q reduces the phase noise, but also decreases the available tuning range. Coupled and single resonators were investigated in this paper and their effect on output power, efficiency, tuning range, and phase noise is reported.

II. Combined HEMT/Varactor Monolithic-Microwave Integrated-Circuit Technology

The VCO wafers were fabricated by the GaAs IC Prototyping Facility [6], Commonwealth Scientific and Industrial Research Organization (CSIRO), Marsfield, N.S.W., Australia, using a combination of existing pulse-doped pseudomorphic HEMT (pHEMT) and Schottky-varactor-diode monolithic-microwave integrated-circuit (MMIC) technologies. This process and the epitaxial material were specially developed for this work. Active layers for the HEMT and varactor devices were sequentially grown on semi-insulating GaAs wafers using a molecular beam epitaxy (MBE) system. Fig. 1 shows a schematic representation of the active layers in the VCO process. The varactor layers were grown on top of the HEMT layers.

The unwanted area of the active layers was etched away to define the HEMT and varactor devices, and also to expose the semi-insulating GaAs substrate on which the microstrip circuitry was to be fabricated. The etching process was carried out in two major steps. The first step was to use reactive ion etching (RIE) to define the varactor mesas. A combination of RIE and wet etching in the second step isolated the HEMT's and the varactors. Fig. 2 shows a schematic cross-sectional view of the HEMT and varactor devices. The connection between the varactor Schottky contact and the microstrip circuit consisted of an air bridge, which crossed the ohmic contact (cathode) surrounding the Schottky contact (anode). Details of the varactor structure have been described previously [7]. The passive circuitry included microstrip transmission lines, thin-film resistors, thin-film capacitors, and air bridges. The wafers

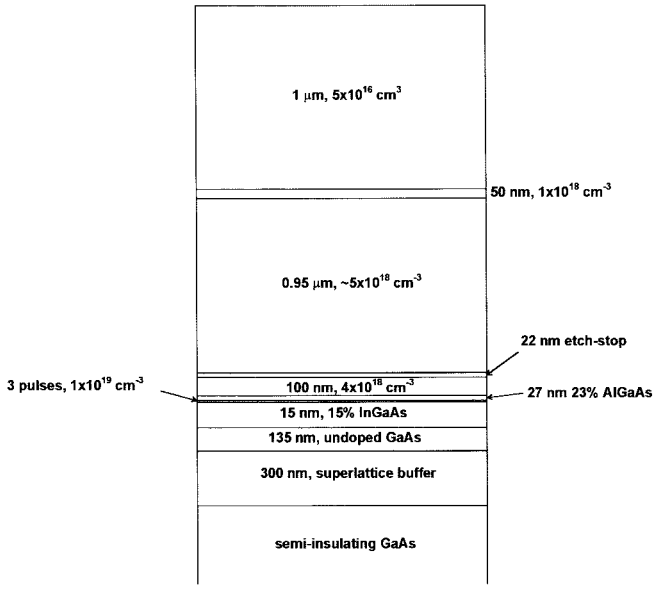

Fig. 1. Schematic structure of the epitaxial layers in the VCO process.

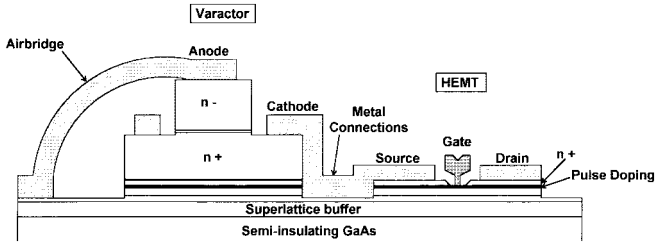

Fig. 2. Schematic cross-sectional view of the HEMT and varactor layers in the combined VCO process.

were thinned to 100 μm. Etched and plated 70-μm-diameter via holes provided ground connection. The mushroom cross-section gates of the HEMT devices were T-shaped, 250-μm wide, and 0.25-μm long. The varactor devices had square Schottky contacts, the size of which was adjusted to suit the operating frequency as described below.

III. Device Models

The circuit performance was simulated using commercial harmonic-balance-analysis software HP-MDS. The active- and passive-device models of HP-MDS were adjusted to represent the measured characteristics of the individual devices. Thin-film resistors included the distributed effects of the resistive film and were modeled using a sheet resistance value of 40-Ω per square. Thin-film capacitors included the distributed effects of the bottom conductor and air-bridge connection to the top metal. The capacitor dielectric was SiO and was modeled with relative permittivity of 5.53 and thickness of 0.26 μm. The microstrip transmission lines and the air bridges were modeled using HP-MDS's microstrip and ribbon elements, respectively, using the bulk conductivity of gold and 2-μm thickness.

A. Varactor Model

The varactor device was modeled as a nonlinear Schottky diode with half-power dependence of capacitance on the reverse anode bias. Varactor test devices were measured on-wafer and the model parameters were extracted from the dc current versus voltage (dc *I–V*) data and the 1–26-GHz bias-dependent s-parameter data. The nonlinear diode model parameters for a varactor device with 26-μm-square anode specific to the VCO wafers were as follows:

1) zero voltage capacitance $C_{jo} = 0.505$ pF;
2) series resistance $R_s = 1.3\ \Omega$;
3) built-in voltage $V_j = 0.8$ V;
4) ideality factor $\eta = 1.04$.

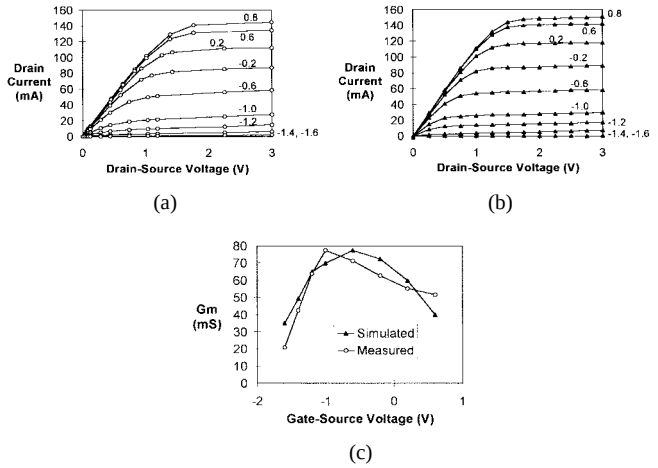

Fig. 3. Drain-current versus drain–source-voltage curves of (a) measured and (b) simulated HEMT device. Measured and simulated transconductance (g_m) of the HEMT device (c) $V_{\rm DS} = 3$ V.

B. HEMT Model

The Curtice cubic-MESFET model [8] available in HP-MDS was used to describe the nonlinear behavior of the HEMT device. To the authors' knowledge, this model is the best approximation to HEMT large-signal performance currently available in the commonly used commercial simulators, and is easily transferable between them. The model parameters were extracted from the dc *I–V* data and the 1–50-GHz bias-dependent s-parameters obtained from on-wafer measurements of test devices. In this model, the gate–source junction is represented as a nonlinear diode with half-power dependence of capacitance on reverse gate bias. This is, at best, an approximation because the gate–source capacitance in an HEMT is not well described by a response of this type as the device approaches pinchoff. The gate–drain-junction capacitance was assumed constant in the HEMT model, a valid assumption for drain voltages above the knee in the dc *I–V* response. The measured drain current of a test device on a VCO wafer is plotted against the drain–source voltage in Fig. 3(a) with gate–source voltage as the varying parameter. Fig. 3(b) shows a similar plot for the HEMT model for the best fit we could achieve. The nonlinear model parameters for this fit is given in Table I. In Fig. 3(c), the measured and simulated transconductance (g_m) is shown as a function of gate–source voltage at a drain voltage of 3 V.

The $1/f$ noise of the HEMT and varactor diode devices was not measured at the time the circuits were designed due to lack

TABLE I
CURTIS-CUBIC MESFET MODEL PARAMETERS USED TO APPROXIMATE THE HEMT DEVICE

β_2=0.011075	R_{IN}=0.006883 Ω	R_G=11.06381 Ω	V_{BI}=0.8 V
R_{DS0}=730.3027 Ω	R_F=0 Ω	R_D=3 Ω	$I_S=10^{-14}$ A
V_{DS0}=0.5 V	F_C=0.11	R_S=3.68 Ω	X_{TI}=3
V_{DSDC}=3.54603 V	C_{GS0}=0.318 pF	L_G=0.037297 nH	E_G=0.69 eV
τ=1.53 psec	C_{GD}=0.018749 pF	L_D=0.027486 nH	η=1.1
γ=3.7		L_S=0.00748 pH	
A_0=0.13925		C_{DS}=0.083943 pF	
A_1=0.070992		C_{RF}=10 pF	
A_2=-0.06247		R_C=269 Ω	
A_3=-0.03274			

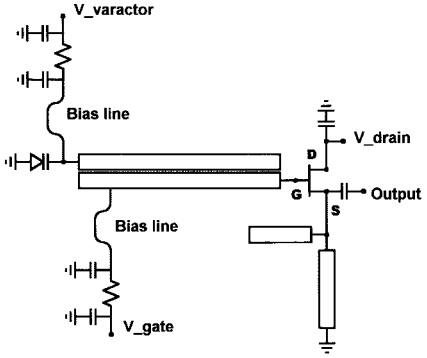

Fig. 4. Schematic circuit diagram of the VCO circuit with a $\lambda/4$ coupled microstrip resonators.

of low-frequency measuring equipment and, hence, were not included in the models.

IV. DESIGN

The VCO circuits were designed for a 50-Ω load using the negative-resistance approach. The HEMT devices were connected in common drain configuration. Gate, drain, and varactor biases were provided separately by $\lambda/4$ microstrip transmission lines. The output was taken from the HEMT source electrode. Open- and short-circuited stubs were connected to the source electrode, provided matching- and second-harmonic suppression. The HEMT devices were biased at maximum g_m, and all three designs were optimized for maximum and uniform output power throughout the frequency tuning range. Schematic circuit diagrams of the VCO's are shown in Figs. 4 and 5 for coupled and single microstrip resonators, respectively.

The first VCO design (VCO type I) incorporated two $\lambda/4$-long coupled microstrip resonators and was designed to operate at approximately 30 GHz. A microphotograph of this circuit is shown in Fig. 6(a). The chip size was 2 mm × 1.75 mm. The varactor anode area was chosen as 18 × 18 μm^2 to give the correct operating frequency at a varactor bias of 2 V.

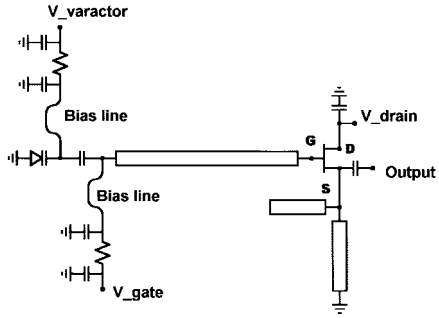

Fig. 5. Schematic circuit diagram of the VCO circuit with a $\lambda/4$ single microstrip resonators.

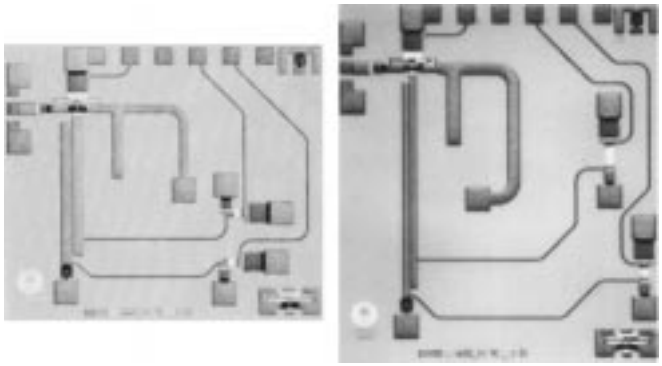

(a) (b)

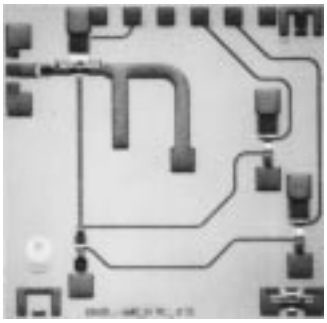

(c)

Fig. 6. Microphotographs of the fabricated (a) VCO type I, designed for 30 GHz. (b) VCO type II and (c) VCO type III, designed for 20 GHz.

VCO types II and III were designed to operate at approximately 20 GHz, and incorporated $\lambda/4$-long coupled and single resonators, respectively. Microphotographs of the fabricated VCO types II and III are shown in Fig. 6(b) and (c). Respective chip sizes were 2 mm × 2.2 mm and 2 mm × 1.95 mm. The varactor anode size was 26 × 26 μm^2 in both circuits.

The simulated oscillation frequency and output power with varying varactor bias are shown in Figs. 7–9, together with the measured performance of typical devices.

V. MEASURED PERFORMANCE

All three designs were included on a single mask set and were fabricated on a 14-mm-square GaAs wafer piece. Power,

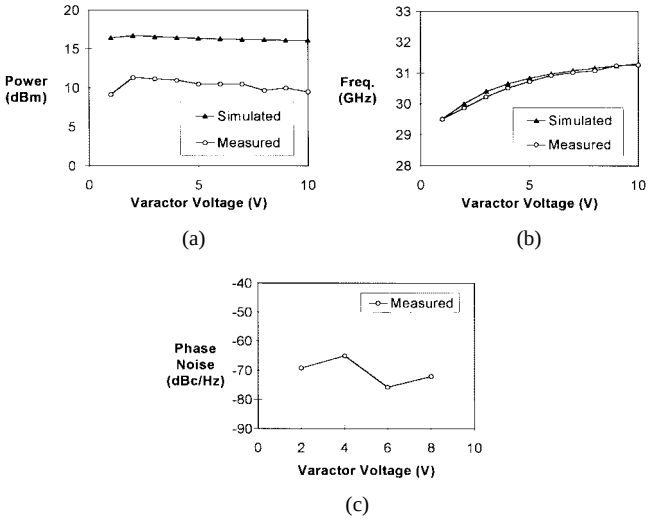

Fig. 7. (a) Simulated and measured output power and (b) frequency together with the (c) measured phase noise of the fabricated VCO type I. The phase noise was measured at 100-kHz offset from the carrier.

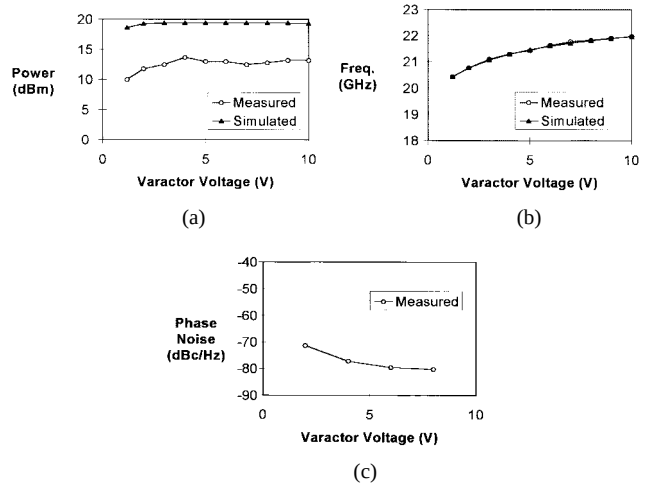

Fig. 8. (a) Simulated and measured output power and (b) frequency, together with the (c) measured phase noise of the fabricated VCO type II. The phase noise was measured at 100-kHz offset from the carrier.

frequency, and phase-noise measurements were carried out using an HP 8564E spectrum analyzer. The phase noise was measured at 100 kHz from the carrier.

Five successful VCO circuits of type I (30-GHz coupled resonator) were prototyped. The measured performance of a typical circuit and the simulated performance using the model parameters derived from the measurements on the same wafer are shown in Fig. 7. The maximum variation in the output power from circuit to circuit on this wafer was 2.3 dB. The 5.4–7.3-dB disagreement observed between predicted and measured power output may be due to inaccuracy of the Curtis-cubic MESFET model in representing the HEMT device. Alternatively, the harmonic-balance-simulation method may not be accurate, and a time-domain approach may give better results. Future work will further investigate the reasons for this disagreement.

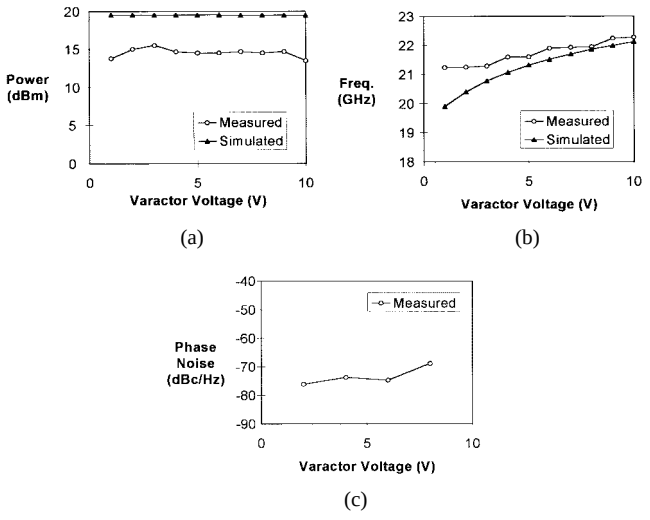

Fig. 9. (a) Simulated and measured output power and (b) frequency, together with the (c) measured phase noise of the fabricated VCO type III. The phase noise was measured at 100-kHz offset from the carrier.

TABLE II
SUMMARY OF MEASURED PERFORMANCE OF THREE VCO DESIGNS. EFFICIENCY AND PHASE NOISE ARE GIVEN FOR THE SPOT FREQUENCIES OF MAXIMUM OUTPUT POWER

VCO Type	Freq. Range (GHz)	Max. Output Power (dBm)	DC to RF Efficiency (%)	Phase Noise at 100KHz (dBc/Hz)
I (coupled)	28.7-31.0	+11.8	7.5	-66.0
II (coupled)	20.4-22.0	+13.7	15.6	-80.3
III (single)	21.2-22.3	+15.5	23.7	-74.7

The measured oscillation frequency versus varactor voltage was in very good agreement with the simulation. The measured frequency varied smoothly throughout its full range, and showed no evidence of frequency hopping. The variation in frequency from circuit to circuit was 0.92 GHz for the same varactor bias voltage. The measured phase noise at 100 kHz varied from −62.2 to −75.8 dBc/Hz.

The measured and simulated performance of the fabricated 20-GHz VCO circuits of types II and III are shown in Figs. 8 and 9, respectively. The VCO type II with a coupled resonator showed similar performance to the VCO type I. The measured power was lower than the prediction by 5.7–8.6 dB, while the oscillation frequency was in good agreement with the prediction. The measured phase noise at 100 kHz varied between −71.3 and −80.3 dBc/Hz. The VCO type III with the single resonator showed slightly different behavior. The power prediction was 4.0–6.0 dB higher than the measurement and dc-to-RF efficiency was higher, but, contrary to expectations, the frequency tuning range was lower than for the coupled resonator case. The measured phase noise at 100 kHz varied from −68.8 to −76.1 dBc/Hz, on average, higher than for the coupled resonator case.

The agreement between the measured and simulated performance is acceptable considering that the nonlinear model used

to describe the HEMT was actually a MESFET model, and the circuits were fabricated using a developmental process.

The overall measured performance of the circuits is comparable to or better than that achieved with other fully monolithic HEMT VCO's, which use alternative methods of frequency tuning. Measured frequency, power, efficiency, and phase noise of the best performing VCO circuit of each type (from the same wafer) are shown in Table II. The output power level shown is the maximum level achieved for each oscillator. The dc-to-RF conversion efficiency and the phase-noise figures are given at the frequencies for the maximum power condition. For the two oscillators at 20 GHz, the one with the single resonator showed the higher efficiency, while the oscillator with the coupled resonator had wider frequency range.

VI. Conclusion

For the first time, fully monolithic VCO circuits using a combined pulse-doped pHEMT and Schottky-varactor diode technology have been designed, prototyped, and tested. These circuits operate at approximately 20 and 30 GHz. Comparison of predicted and measured output power and frequency indicated that only the frequency predictions were accurate. The measured performance of coupled- and single-resonator oscillators was compared. Better efficiency was achieved with the single-resonator oscillator, while the coupled-resonator oscillators were found to produce lower phase noise and, contrary to expectations, a wider frequency coverage.

Acknowledgment

The authors thank R. A. Batchelor for valuable discussions on the measurements, and J. Wiggins, R. Chai, M. Vaughan, Z. Kachwalla, and F. Ceccato for producing the VCO wafers.

References

[1] I. D. Robertson, Ed., *MMIC Design* (Inst. Elect. Eng. Circuits and Systems Series 7). London, U.K.: IEE, 1995, pp. 337–370.

[2] A. Bangert, M. Schlechtweg, M. Lang, W. Haydl, W. Bronner, T. Fink, K. Khöler, and B. Raynor, "W-band MMIC VCO with a large tuning range using a pseudomorphic HFET," in *IEEE MTT-S Int. Microwave Symp. Dig.*, vol. 2, San Francisco, CA, June 18–20, 1996, pp. 525–528.

[3] M. Schefer, U. Lott, H. Benedickter, B.-U. Klepser, W. Patrick, and W. Bächtold, "Monolithic coplanar, varactor tunable V-band HEMT oscillator with injection locking capability," *Electron. Lett.*, vol. 32, pp. 1899–1900, Sept. 1996.

[4] P. Gardner, D. K. Paul, and K. P. Tan, "Microwave voltage tuned microstrip ring resonator oscillator," *Electron. Lett.*, vol. 30, pp. 1770–1771, Oct. 1994.

[5] V. Güngerich, F. Zinkler, W. Anzill, and P. Russer, "Noise calculations and experimental results of varactor tunable oscillators with significantly reduced phase noise," *IEEE Trans. Microwave Theory Tech.*, vol. 43, pp. 278–285, Feb. 1995.

[6] G. J. Griffiths and J. W. Archer, "Australian MMIC prototyping in the 40, 60 and 90 GHz bands," in *Proc. IEEE Asia–Pacific Microelectron. Conf.*, Nov. 1995, pp. 448–451.

[7] J. W. Archer, R. A. Batchelor, and C. J. Smith, "Low-parasitic, planar Schottky diodes, for millimeter-wave integrated circuits," *IEEE Trans. Microwave Theory Tech.*, vol. 38, pp. 15–22, Jan. 1990.

[8] W. Curtice and M. Ettenberg, "A nonlinear GaAs FET model for use in the design of output circuits for power amplifiers," *IEEE Trans. Microwave Theory Tech.*, vol. 33, pp. 1383–1394, Dec. 1983.

Oya Sevimli (M'89) was born in Ankara, Turkey, in 1960. She received the B.Sc. and M.Sc. degrees in electrical and electronics engineering from the Middle East Technical University (METU), Ankara, Turkey, in 1981 and 1985, respectively.

From 1981 to 1986, she was a Research Assistant at METU. In 1987, she joined the Telecommunications and Industrial Physics Division, Commonwealth Scientific and Industrial Research Organization (CSIRO), Marsfield, N.S.W., Australia. Since that time, she has designed many novel GaAs MMIC's for frontier research on microwave and millimeter-wave circuits and systems. She is currently working on new MMIC designs on GaAs and InP materials, and managing the MMIC Packaging Facility, CSIRO.

John W. Archer (M'82–SM'83–F'90) was born in Sydney, Australia, in 1950. He received the B.Sc., B.E. (Hons. I) and Ph.D. degrees from Sydney University, Sydney, N.S.W., Australia, in 1970, 1972, and 1977, respectively.

His professional career has been distinguished by sustained contributions to the development of millimeter-wave technology. His Ph.D. research led to the world's first 100-GHz variable-baseline two-element coherent interferometer for radio astronomy. From 1977 to 1984, he was with NRAO, where his research focused on millimeter-wave systems for radio astronomy; particularly, component design and receiver construction. During this period, he gained international recognition for his work on the development of frequency multipliers, fixed-tuned mixers, and novel cryogenic receivers. In 1984, he was appointed to head a new research group at the Commonwealth Scientific and Industrial Research Organization (CSIRO), Marsfield, N.S.W., Australia. Over the last 14 years, he has successfully established an Australian resource base in GaAs MMIC technology, which has lead to the application of this technology in the Australian Defense and telecommunications industries. In parallel with this leadership role, he has continued to contribute to the development of new millimeter-wave MMIC components, highlights of which include the development of unique planar Schottky diodes and MMIC's incorporating them, low-noise MMIC amplifiers of novel design for frequencies from 20 to 100 GHz, including a patented, novel bidirectional amplifier technology and VCO's. He has achieved international recognition for his contributions to millimeter-wave receiver technology. He is on the editorial board of Wiley's *Microwave and Optical Technology Letters*.

Dr. Archer is an editorial board member of the IEEE Transactions on Microwave Theory and Techniques.

Grant J. Griffiths (S'75–M'75) was born in North Wales, U.K., in 1952. He received the B.Sc. degree from the University of Natal, South Africa, in 1974, and the Ph.D. degree for his work in integrated optics from the University of Queensland, Queens., Australia, in 1981.

For the following 18 months, he was with the University of California at Santa Barbara, where he worked on MBE technology and novel III–V device structures. This was following by 18 months with AT&T Bell Laboratories, Murray Hill, NJ, where he designed and constructed a custom MBE facility for epitaxial growth of dielectrics on InP. Since 1984, he has been with the Commonwealth Scientific and Industrial Research Organization (CSIRO) Telecommunications and Industrial Physics, Marsfield, N.S.W., working in MBE, device, and process development. He is currently Manager of the CSIRO GaAs IC Prototyping Facility, which is an R&D-level MMIC foundry for the microwave and millimeter-wave communications and defense industries. His major contribution to what has become recognized as a world-class activity in this area has been the development of novel material and device structures for operation at millimeter-wave frequencies.